International Conference on Applied Energy 2019
Aug 12-15, 2019, Västerås, Sweden
Paper ID: # 443

Centrifugal Granulation of Molten BF Slag in Film Formation Mode During Waste Heat Recovery Process

Yu Tan[1,2], Xun Zhu[1,2*], Hong Wang[1,2], Yi-Wen Lv[1,2], Xian-Yan He[1,2], Qiang Liao[1,2]
1 Key Laboratory of Low-grade Energy Utilization Technologies and Systems, Chongqing University, Chongqing 400030, China
2 Institute of Engineering Thermophysics, Chongqing University, Chongqing 400030, China

ABSTRACT

Molten blast furnace (BF) slag is discharged at high temperature during the iron-making process, and contains a high content of thermal energy. Traditional water quenching methods fail to recover this thermal energy. Hence, a number of dry granulation heat recovery techniques were proposed, and reducing the particle size is regarded as the key route to improving heat recovery efficiency. Among all the proposed techniques, the centrifugal granulation method is recognized as the most promising. In this paper, the centrifugal granulation characteristics for molten BF slag in film formation mode were experimentally studied. The effect of the rotating speed, the molten slag mass flow rate and the slag initial temperature on the particle size are discussed. The results show that an unusual histioid type of film disintegration phenomenon occurs during the granulation process, which is beneficial to the fragmentation of the film. Furthermore, a higher rotating speed and a smaller slag flow rate contribute to the reduction of particle size. The present study provides guidance for improving granulation heat recovery performance for molten BF slags in industrial applications.

Keywords:
Molten slag; Thermal energy recovery; Centrifugal granulation; Film formation mode

NONMENCLATURE

Abbreviations	
BF	*Blast furnace*
Symbols	
d_a	*Overall average diameter of particles*
d_i	*Average diameter of particles in each individual size range*
N	*Atomizer rotating speed*
Q_m	*Mass flow rate of molten BF slag*
R_c	*Granulation chamber radius*
θ_i	*Mass fraction of particles in each individual size range*
ρ	*Density of molten BF slag*
μ	*Viscosity of molten BF slag*
σ	*Surface tension of molten BF slag*

1. INTRODUCTION

Molten blast furnace (BF) slag is produced in pig iron making processes with a high temperature of 1450-1650 °C [1]. The thermal energy in molten BF slag accounts for 25% of all the high temperature waste heat in the steel-making industry [2]. Traditional water quenching methods achieve only a fast cooling of molten BF slag to yield a high vitreous content product, which is used for cement production [3]. However, most of the thermal energy carried by the molten BF slag is wasted.

In order to recover the thermal energy in molten BF slag, a number of dry granulation techniques, combined with methods for heat recovery were proposed, e.g., the centrifugal granulation, rotating drum and air blast techniques [4]. Recently, centrifugal granulation has received a great deal of attention, and is generally accepted as the most promising technique by virtue of its simple and compact structure, energy conservation and smaller particle size [5].

Mizuochi et al. [6] conducted experiments to verify the feasibility of centrifugal granulation for molten slag. Subsequently, Purwanto et al. [7], Liu et al. [8] and Chang et al. [9] investigated the granulation characteristics of molten slag in drop formation and ligament formation mode. Furthermore, Zhu et al. [10, 11] observed the granulation phenomena in both ligament and film formation mode, and the effect of the rotating speed on the particle size was characterized. However, most of the above studies focused on the granulation characteristics in ligament formation mode. In industrial scale applications, however, the film formation mode is considered to be the most suitable mode, due to its capacity to support a larger molten slag mass flow rate. Despite this, the effects of pivotal factors such as molten slag mass flow rate and slag initial temperature on the granulation characteristics in film formation mode are still unknown.

In the present study, granulation was maintained in film formation mode. The fragmentation phenomenon of film was investigated and the effects of rotating speed, molten slag mass flow rate and slag initial temperature on the granulation characteristics are studied and discussed.

2. EXPERIMENTAL SYSTEM AND METHODS

2.1 Experimental apparatus

The experiment system is illustrated in Fig 1. A high temperature resistance furnace was placed at the top. Inside the furnace, a graphic crucible was set in the middle to hold the melted molten BF slag. In order to realize the discharging of molten slag, a hole was designed in the bottom of the graphic crucible. A stopper was used as a switch to control the beginning and ending of the discharging process. Beneath the furnace was a granulation chamber. Directly below the discharging pipe, a motor driven rotary cup atomizer was employed to actualize the granulation process. The rotating speed of rotary cup was adjusted by a frequency converter. The diameter of the rotary cup was set as 126 mm, and the detailed structure is shown in Fig 2. A camera was placed at the upper right direction to record the granulation phenomenon. In order to hinder the adhesion of half solidified particles on the inner wall of the granulation chamber when the particles were impacting the surface, an inner water cooling jacket was set inside the granulation chamber and covered a circumferential angle range of 36°. The distance between the inner water cooling jacket and the atomizer was set as 0.68 m. Another outer water cooling jacket outside the granulation chamber was designed to transport the high temperature particles to the collector.

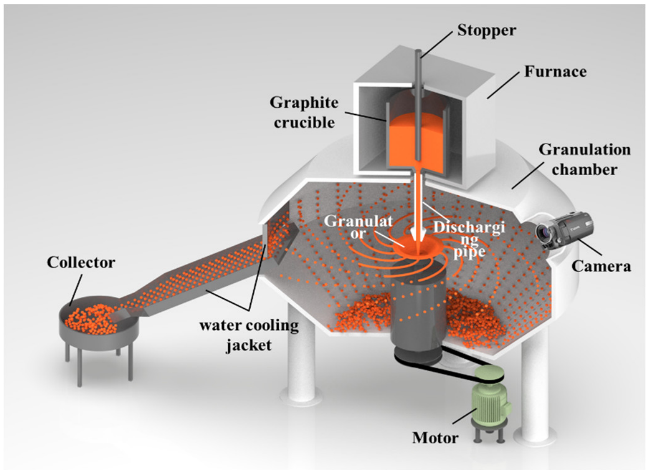

Fig 1 Schematic diagram of molten BF slag centrifugal granulation experimental system.

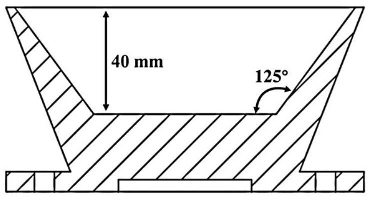

Fig 2 The structure of adopted rotary cup atomizer.

2.2 data processing and working medium

After each experiment, the solidified products in the collector were collected and sieved by a set of standard screens. The particles were defined as the products smaller than 8 mm in diameter, and the products larger than 8 mm were regard as slagging aggregation. The average diameter of granulated particles was calculated by the following equation:

$$d_a = \sum_i^n d_i \theta_i \quad (1)$$

The industrial water quenched BF slag was adopted as the working medium, which was heated to 1400-1500 °C in the high temperature resistance furnace. The main components and physical properties of molten BF slag are provided in Table 1.

Table 1 The main components and physical properties of molten BF slag.

Main components	CaO	SiO_2	MgO	Al_2O_3	TiO_2
	39.2%	30.3%	8.0%	11.3%	5.95%

Temperature (°C)	Density (kg/m^3) [12]	Viscosity (Pa·s)	Surface tension (N/m) [12]
1400	2600	0.535	0.546
1450	2600	0.3186	0.538
1500	2600	0.2163	0.53

3. RESULTS AND DISCUSSION

3.1 *Film formation phenomena and analysis*

In the present work, the mass flow rates of molten BF slag were set above 180 g·s^{-1}, and the fragmentation modes for all the operation conditions were in film formation mode, as illustrated in Fig 3. One can see that a sheet with jagged edge was thrown out from the lip of rotary cup. At the rim of the extended sheet, small holes were generated and gradually expanded. The sheet was then torn into a series of reticular ligaments. Finally, the reticular ligaments were stretched outwards and followed by a strong crushing process to form small droplets. The film formation mode for molten BF slag presented a special histioid type of film disintegration, which was very different from the film disintegration phenomenon for other low temperature working fluids.

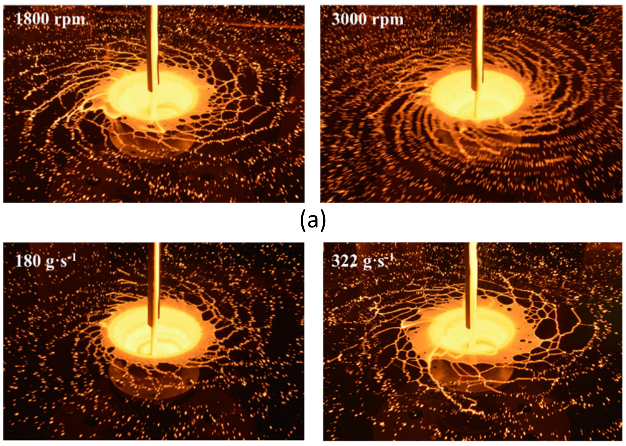

Fig 3 The structure of adopted rotary cup atomizer; (a)Q_m=280 g·s^{-1}, (b)N=1800 rpm.

We have been given an insight into the micro morphology of a single granulated particle, which showed that particle has an internal micro-bubble filling structure with scales of dozens of microns [10]. It can be deduced that the micro-bubble filling structure of molten BF slag leads to the emergence of histioid type disintegration.

3.2 *Effect of rotating speed*

The effect of rotating speed on the average particle diameter and slagging mass fraction is displayed in Fig 4. It can be seen from Fig 4(a) that the average particle diameter decreased significantly with the increase of rotating speed. At higher rotating speed, the strong disturbance effect of the surrounding air on the sheet as well as the enhanced centrifugal force lead to a more violent film rupture process, thus greatly reducing the particle size. The variation of slagging mass fraction illustrated in Fig 4(b), shows that the slagging mass fraction decreased dramatically with increasing rotating speed at small rotating speed conditions. When the rotating speed was increased above a certain value (around 1200 rpm), on the other hand, the decline in the rate of slagging mass fraction was relatively minor .

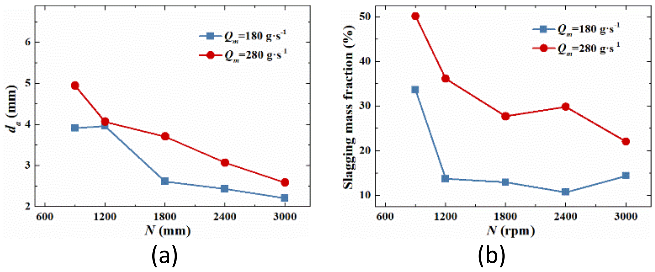

Fig 4 Effect of rotating speed on (a) average particle diameter, (b) slagging mass fraction.

3.3 *Effect of molten slag mass flow rate*

The effect of molten slag mass flow rate on the average particle diameter, as illustrated in Fig 5(a), one can see that the average particle diameter first increased rapidly with an increase in molten slag mass flow rate up to around 300 gs^{-1}, beyond which only small increases were seen. Fig 5(b) shows the effect of molten slag mass flow rate on the slagging mass fraction. It is noted that the slagging mass fraction increased approximately linearly with increasing molten slag mass flow rate. At Q_m= 609 g·s^{-1}, the slagging mass fraction reached 76%, which indicated that most of the slag droplets were sticking together and formed slagging aggregation on the surface of the water cooling jacket during the impacting process.

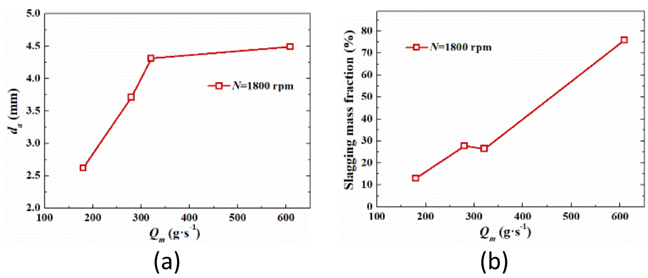

Fig 5 Effect of molten slag mass flow rate on (a) average particle diameter, (b) slagging mass fraction.

3.4 *Effect of slag initial temperature*

Fig 6(a) shows the effect of slag initial temperature on the average particle diameter. One can see that the variation ranges of average particle diameter were quite small; thus, the slag initial temperature had a negligible influence on the granulation performance. However, the slagging mass fraction curves in Fig 6(b) demonstrate that a lower slag initial temperature was beneficial to the suppressing of slagging. As such, 1400 °C is regarded as the best slag initial temperature condition for centrifugal granulation.

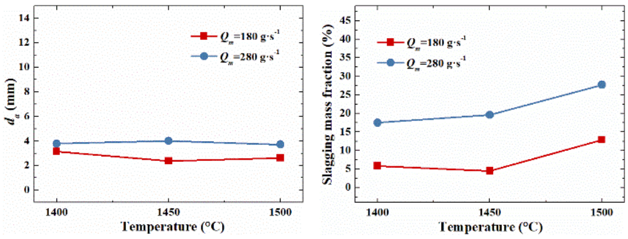

(a) (b)

Fig 6 Effect of slag initial temperature on (a) average particle diameter, (b) slagging mass fraction.

4. CONCLUSIONS

In the present study, the centrifugal granulation characteristics of molten BF slag in film formation mode were specifically investigated. The main findings are as follows:

(1) The special histioid type of film disintegration in film formation mode was mainly caused by the micro-bubble filling structure inside the molten BF slag. The histioid type of disintegration is beneficial to improving the film rupture process.

(2) The average particle diameter decreased with an increase in rotating speed and a decrease in the molten slag mass flow rate. A larger molten slag mass flow rate should be matched with a higher rotating speed.

(3) The effect of slag initial temperature on particle size can be neglected. A lower slag initial temperature was effective in suppressing slagging. A temperature of 1400 °C is regarded as the best slag initial temperature condition.

ACKNOWLEDGEMENT

The author would like to thank the National Key R&D Program of China (No. 2017YFB0603602), the Project No. 106112017CDJRTY0108 supported by the Fundamental Research Funds for the Central Universities and the Venture & Innovation Support Program for Chongqing Overseas Returnees (cx2018053).

REFERENCES

[1] Bisio G. Energy recovery from molten slag and exploitation of the recovered energy[J]. Energy, 1997, 22(5): 501-509.

[2] Zhang H, Wang H, Zhu X, et al. A review of waste heat recovery technologies towards molten slag in steel industry[J]. Applied Energy, 2013, 112: 956-966.

[3] Song H W, Saraswathy V. Studies on the corrosion resistance of reinforced steel in concrete with ground granulated blast-furnace slag—an overview[J]. Journal of hazardous materials, 2006, 138(2): 226-233.

[4] Yu P, Wang S, Li Y, et al. A Review of Granulation Process for Blast Furnace Slag[C]//MATEC Web of Conferences. EDP Sciences, 2016, 68: 06007.

[5] Wang H, Wu J J, Zhu X, et al. Energy–environment–economy evaluations of commercial scale systems for blast furnace slag treatment: dry slag granulation vs. water quenching[J]. Applied energy, 2016, 171: 314-324.

[6] Mizuochi T, Akiyama T, Shimada T, et al. Feasibility of rotary cup atomizer for slag granulation[J]. Isij International, 2001, 41(12): 1423-1428.

[7] Purwanto H, Mizuochi T, Tobo H, et al. Characteristics of glass beads from molten slag produced by rotary cup atomizer[J]. Materials transactions, 2004, 45(12): 3286-3290.

[8] Liu J, Yu Q, Duan W, et al. Experimental investigation on ligament formation for molten slag granulation[J]. Applied thermal engineering, 2014, 73(1): 888-893.

[9] Chang Q, Li X, Ni H, et al. Modeling on dry centrifugal granulation process of molten blast furnace slag[J]. ISIJ International, 2015, 55(7): 1361-1366.

[10] Tan Y, Zhu X, Wang H, et al. Centrifugal granulation characteristics of molten blast furnace slag and performance of the granulated particles[J]. Applied Thermal Engineering, 2018, 142: 683-694.

[11] Tan Y, Zhu X, He X Y, et al. Granulation characteristics of molten blast furnace slag by hybrid centrifugal-air blast technique[J]. Powder Technology, 2018, 323: 176-185.

[12] Kashiwaya Y, In-Nami Y, Akiyama T. Mechanism of the formation of slag particles by the rotary cylinder atomization[J]. ISIJ international, 2010, 50(9): 1252-1258.